www.sciencemag.org/cgi/content/full/1142834/DC1

Supporting Online Material for

Free-Drifting Icebergs: Hot Spots of Chemical and Biological Enrichment in the Weddell Sea

Kenneth L. Smith Jr.,* Bruce H. Robison, John J. Helly, Ronald S. Kaufmann, Henry A. Ruhl, Timothy J. Shaw, Benjamin S. Twining, Maria Vernet

*To whom correspondence should be addressed. E-mail: ksmith@mbari.org

Published 21 June 2007 on *Science* Express

DOI: 10.1126/science.1142834

This PDF file includes:

Supporting Online Material

Iceberg dynamics

Aerial measurements of each iceberg were determined using a laser-ranging device combined with an integrated, high-precision GPS unit and continuously derived ship-track data. For iceberg density estimates, a SCANSAR/Wideband image (#R15378) taken on 22 February 2006 was obtained from the Alaska Satellite Facility. The image was georeferenced and visualized in GRASS and Adobe Photoshop. The image was converted to tif format and a sub-region extracted using Photoshop, as a region visually free of pack ice with only free-drifting icebergs. The extracted image was loaded into MATLAB and processed by estimating the background, subtracting it from the image, thresholding the result using a subjective cutoff, converting the image to binary (black/white), and counting the white objects. This process followed the example of counting rice grains presented in the image processing toolbox manual that is part of the MATLAB documentation. This technique worked well using a structuring value of 200 pixels for background subtraction. Each pixel was 50 x 50 m in the source imagery, and the smallest object counted, after grayscale thresholding, was 2 x 2 pixels, i.e. 100 x 100 m.

Nutrient analysis

Nutrient concentrations were determined by flow injection analysis using a Lachat Instruments Quikchem 8000 autoanalyzer. Samples were collected directly from the rosette Niskin bottles; samples not processed at time of collection were frozen and stored at -20ºC until analysis (performed within a few days). The phosphate method was a modification of the molybdenum blue procedure of Bernhardt and Wilhelms (*1*), in which

phosphate was determined as reduced phosphomolybdic acid employing hydrazine as the reductant. The nitrate + nitrite analysis used the basic method of Armstrong et al. (*2*), with modifications to improve the precision and ease of operation. Sulfanilamide and N-(1-Napthyl)ethylenediamine dihydrochloride reacted with nitrite to form a colored diazo compound. For the nitrate + nitrite analysis, nitrate was first reduced to nitrite using a cadmium reduction column and imidazole buffer as described by Patton (*3*). The silicic acid method was based on that of Armstrong et al. (*2*) as adapted by Atlas et al. (*4*). Addition of an acidic molybdate reagent formed silicomolybdic acid which was then reduced by stannous chloride. Ammonia was determined by an indophenol blue method modified from ALPKEM RFA methodology which references Methods for Chemical Analysis of Water and Wastes, March 1984, EPA-600/4-79-020, "Nitrogen Ammonia", Method 350.1 (Colorimetric, Automated Phenate).

Radioisotope analysis

Surface samples were obtained from the ship's clean seawater system, stored in either 200 L polyethylene barrels or 1000 L tanks and later pumped at ~1L min^{-1} through Mn-fiber columns to extract Ra and Th. The Mn-fibers, containing extracted radionuclides, were rinsed with de-ionized water, partially dried, and placed in a circulation/counting system (*5*). Helium was circulated over the Mn-fiber to sweep ^{219}Rn and ^{220}Rn generated by ^{223}Ra and ^{224}Ra decay through a scintillation cell. Signals generated by alpha particles from the decay of Rn and daughters were recorded and routed to a delayed coincidence system for Ra measurements. The delayed coincidence system utilizes the difference in decay constants of the short-lived daughters to uniquely

determine the activity associated with ^{223}Ra and ^{224}Ra on the Mn fiber. Samples were measured (counted) a total of three times over the 3-month period following collection to monitor the equilibration of ^{224}Ra and ^{223}Ra with their parent isotopes ^{228}Th and ^{227}Ac. Excess ^{224}Ra was derived from the difference between the measured ^{224}Ra and ^{228}Th, assuming the uptake efficiency of each was 100%.

Phytoplankton

Water samples were collected around the icebergs and in iceberg-free waters via rosette/Niskin bottles from the ship. Concentrations of chlorophyll-*a* were estimated fluorometrically (*6*). Water aliquots were filtered onto individual filters, frozen at -80^{o} C for at least 24 h, extracted in 90 % acetone at -20^{o} C and concentrations measured with a digital Turner Designs fluorometer Model AU10. Calibration was done with pure chlorophyll (commercially available). Chlorophyll was measured in 5 size fractions: 0.22, 0.7 (Whatman GF/F), 3.0, 5.0 and 20.0 µm membrane filters. The underway fluorometry voltage readings were converted to chlorophyll-*a* using the following formula: Chl-*a* = 8.1781(V) – 0.8197.

Iceberg-associated communities

A Phantom DS-2 remotely operated vehicle (ROV) was used to visually examine the submerged flanks and adjacent water of both icebergs. The Phantom is a small ROV that operates with a positively buoyant, soft tether. During dive operations the ship stood off from the iceberg at a safe distance while the ROV was launched and flown, at the surface, to a point near the dive site but outside the surf zone, after which it commenced its

descent. Color video feed, including graphic overlays of compass heading and depth, were monitored and recorded throughout the dives at the shipboard control station. While the ROV tether was too short to allow inspection of the undersides of the icebergs, we were able to examine the submerged vertical faces down to 150 m and the undercut leading to their undersides, down to about 200 m. The ROV was fitted with a modified ¼ m diameter plankton net that was scraped along the ice surface to collect biological and geological samples. A total of six dives were made, ranging from 1.5 to 3.2 hours in duration.

Zooplankton/micronekton

Macrozooplankton and micronekton were collected using a six-net MOCNESS trawl with a 10 m^2 mouth opening. Each net had 4-mm circular mesh in the body and 505-µm mesh cod ends (*7*). Samples were collected at distances of 0.19, 0.37, 0.93, 1.9, 3.7, and 9.3 km from each iceberg. For the smaller iceberg, W-86, trawling was executed in a spiral pattern, with complete circuits at the distances listed above (*e.g.* circuit at 0.19 km distance, followed by a circuit at 0.37 km, etc.). For the larger iceberg, A-52, trawling was conducted along the lengths of both sides of the iceberg (*e.g.* linear transect at 0.19 km distance, followed by a linear transect at 0.37 km, etc.). During each circuit or linear transect, the trawl was towed at an average speed of *ca.* 2 knots in a "tow-yo" fashion, *i.e.* lowering the MOCNESS to $\leq$ 500 m and bringing it back to just below the surface for each net. All trawl deployments were conducted within several hours before and after local noon during austral spring when day length exceeded 18 hours. Each net of the MOCNESS was open for approximately one hour.

After retrieval of the trawl, samples were sorted on ice to lowest identifiable taxon and counted. Sorted samples were blotted dry, and displacement volume was measured to the nearest 0.1 ml using a graduated cylinder. After displacement volume measurements were completed, all samples were preserved in 3.7% buffered formalin. In the case of euphausiids and fishes, total length was measured for all individuals (fishes) or up to 50 individuals from each sample (euphausiids). Displacement volumes were converted to wet weights, assuming a conversion of 1.0 g ml^{-1}.

Individual krill were selected randomly from 10 m^2 MOCNESS trawl samples collected over a range of distances from W-86 (N = 48) and A-52 (N = 39). For each specimen, the abdomen (gut) was removed, placed in 10 ml of 90% acetone in water, and extracted for 24 h at -20^{o}C. Chlorophyll and phaeopigments were measured by fluorescence, as described above, in units of ng pigment per krill.

Seabirds

Seabird surveys were conducted opportunistically during other activities and transits between stations. Surveys typically were made from the ship's bridge for either 5-min segments or for complete circumnavigations of each iceberg. Distance to each iceberg was measured using the ship's radar, and supplemented with laser ranging, where possible. Relative iceberg position was also recorded for each survey. Effective visibility was estimated to be approximately 0.46 km using the ship's radar plus laser ranging. Surveys were not conducted during heavy snow, fog, and twilight when the visibility dropped below this effective range. The distance traveled during each timed survey was extracted from the ship's navigational records and environmental data from

the ship's underway data. The area sampled was calculated by multiplying the effective strip width by the survey distance. To estimate the effect of distance to each iceberg, densities (counts ha^{-1}) were partitioned into three distance ranges: 'at' (< 0.18 km from the iceberg), 'near' (0.18 to 0.92 km from the iceberg), and 'far' (> 0.92 km from the iceberg). Most birds were highly mobile, and a survey conducted in a fixed position typically sampled many birds that moved through the survey area over a period of several minutes. To address this issue, we evaluated iceberg-related effects in terms of counts min^{-1} of survey time; these results were not significantly different from the 5-min counts m^{-2}. When possible, surveys were conducted every hour, with a total of 165 survey periods, from 0.18 km to greater than 0. 92 km from the nearest iceberg.

Phytoplankton cultures

The centric diatom *Thalassiosira weissflogii* (CCMP 1336) was chosen for the bioavailability experiment. Although isolated from a coastal environment, this species has been used in numerous studies of Fe availability and uptake, and is representative of a class of phytoplankton that comprises a critical component of the export production in the Southern Ocean. A batch culture of *T. weissflogii* was grown in 100 mL of Aquil media (*8*) prepared without metals or EDTA but amended with 1 mg of iceberg sediment (following several rinses with 18-Mohm water). Upon reaching stationary phase ($\sim 4\times10^5$ cells mL^{-1}), cells from this batch culture were collected on a 0.2-µm polycarbonate membrane, rinsed with trace-metal-free synthetic ocean water, and resuspended into Aquil media prepared without metals or EDTA. The resuspended cells were used to inoculate triplicate polycarbonate flasks containing 100 mL of either complete Aquil media, Aquil prepared without metals/EDTA, or Aquil without metals/EDTA but

containing 1 mg iceberg sediment. This sediment load was similar to our estimate of terrigenous input adjacent to the iceberg and on the same order as similar experiments using terrigenous material (*9*). Flasks were acid-washed prior to use and cultures were sampled only in a Class-100 environment using trace-metal clean technique. Media was sterilized by microwave to avoid metal contamination during autoclaving. Cultures were grown at 15ºC under 300 µmol photon m^{-2} s^{-1} using a 14:10 light:dark cycle. Cell density was assayed with a Coulter Multisizer II particle counter.

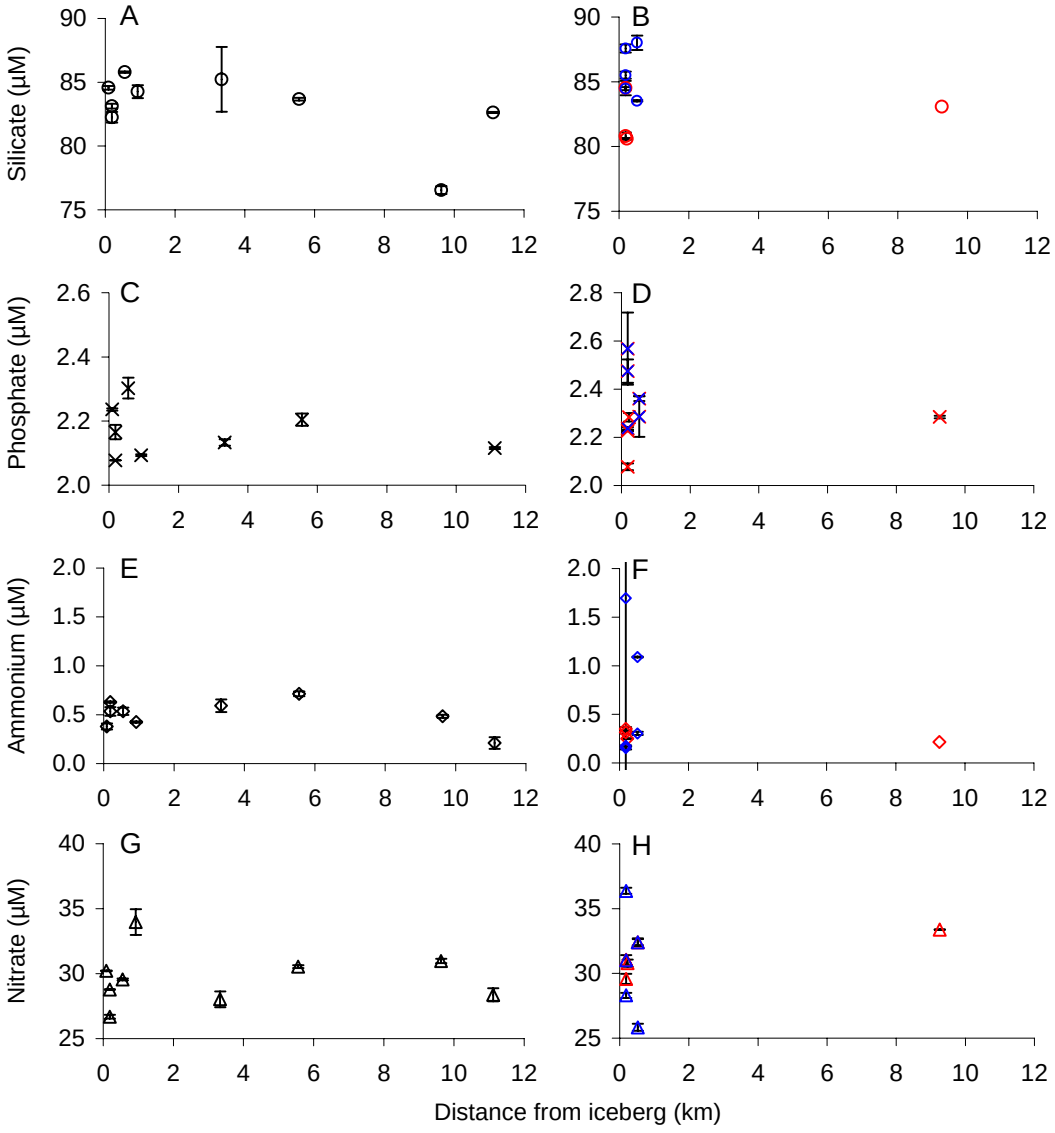

Fig. S1. Mean surface water (± std. error) nutrient concentrations from 1 m and 10 m depth samples taken from 20 m to > 9 km radial distance from icebergs W-86 (n = 9)and A-52 (n = 10). The first and second sampling periods around A-52 are differentiated by blue and red symbols respectively (**A,B**) Silicate determined from water collected with CTD/rosette casts. (**C,D**) Phosphate. (**E,F**). Ammonium. (**G,H**) Nitrate. Higher

variability in all nutrient concentrations was measured during the first sampling period (blue) around A-52.

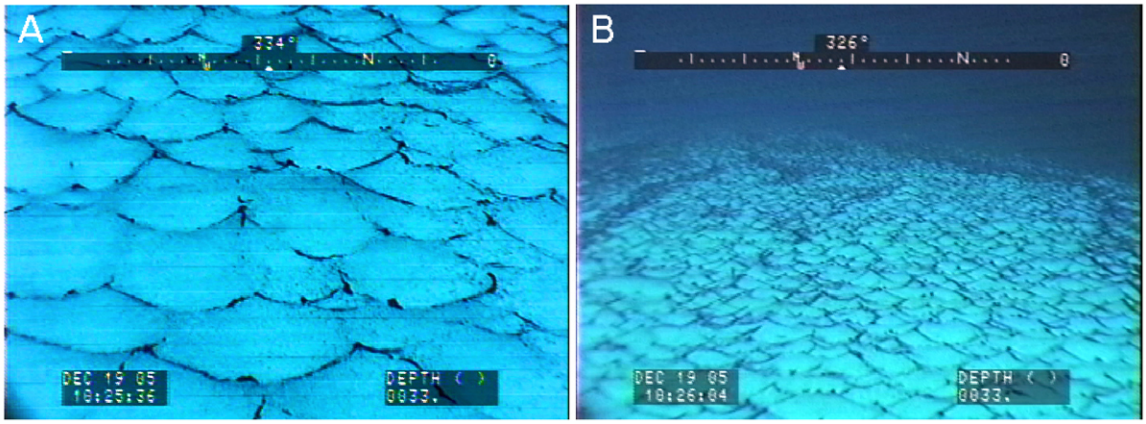

Fig. S2. Algal tufts attached to the circular ridges separating ablation hollows at 10 m depth on a gently sloping shelf that projected horizontally from iceberg A-52 (**A**). The width of the close-up video frame grab is about 30 cm. (**B**) The frame grab on the right encompasses an area of about 1 m^2. All of the dark material on the ice in these images is algae.

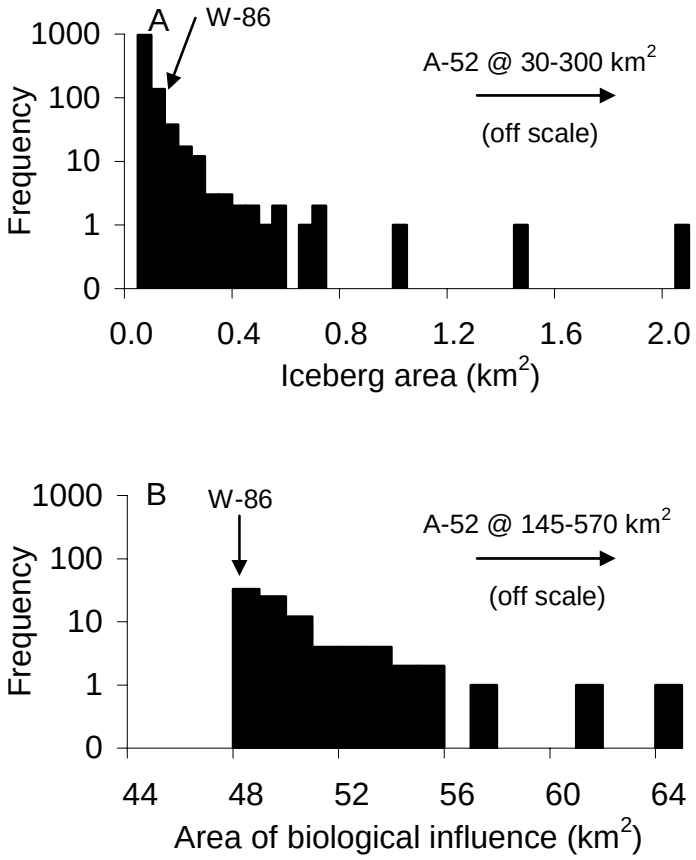

Fig. S3. Iceberg size frequency distribution obtained by processing a RADARSAT SCANSAR/Wideband satellite image (R15378) taken in proximity to our study site in the NW Weddell Sea. (**A**) Size frequency distribution of 962 icebergs identified in 11,265 km^2. Surface areas of W-86 and A-52 are shown for comparison. (**B**) Size frequency distribution of 89 icebergs enhanced with a zone of biological influence to 3.7 km radius that fell within the size range of W-86 and A-52.

Iceberg	Component	near field n	far field n	U	*p* (2-tail)
W86	Chlorophyll-*a*	62	26	346	<0.001
	Macrozooplankton/ micronekton abundance	15	9	58	0.82
	Macrozooplankton/ micronekton displacement vol.	15	9	41	0.41
	Krill gut pigment	38	10	0	<0.001
	Seabird abundance	33	49	17	<0.001
	Seabird community evenness	33	49	215	<0.001
A52 pooled	Chlorophyll-*a*	95	18	560	0.02
	Macrozooplankton/ micronekton abundance	24	6	23	0.009
	Macrozooplankton/ micronekton displacement vol.	24	6	20	0.005
	Krill gut pigment	29	10	169	0.44
	Seabird abundance	52	31	124	<0.001
	Seabird community evenness	52	31	1303	<0.001
A52 first sampling	Chlorophyll-*a*	52	no sample	-	-
	Macrozooplankton/ micronekton abundance	no sample	no sample	-	-
	Macrozooplankton/ micronekton displacement vol.	no sample	no sample	-	-
	Krill gut pigment	no sample	no sample	-	-
	Seabird abundance	32	7	6	<0.001
	Seabird community evenness	32	7	206	<0.001
A52 second sampling	Chlorophyll-*a*	43	18	356.5	0.63
	Macrozooplankton/ micronekton abundance	24	6	23	0.009
	Macrozooplankton/ micronekton displacement vol.	24	6	20	0.005
	Krill gut pigment	29	10	169	0.44
	Seabird abundance	20	24	91	<0.001
	Seabird community evenness	20	24	351	<0.001

Table S1. Statistical comparison of chlorophyll-*a*, macrozooplankton/ micronekton abundance and displacement volume, krill gut pigment, and seabird abundance, and Pielou's evenness in the near- and far-field surrounding icebergs W-86 and A-52 (first and second sampling; combined) using the Mann-Whitney U test. Near-field ≤ 3.7 km radial distance from iceberg, far-field >3.7 km radial distance from iceberg for all components except seabird abundance for which near-field is smaller at ≤ 0.92 km and the far-field is > 0.92 km.

References

1. H. Bernhardt, A. Wilhelms. *Technicon Symp*., 1967, Vol. I, 386 (1967).

2. F.A.J. Armstrong, C. R. Stearns, J. D. H. Strickland. *Deep-Sea Res.* **14**, 381 (1967).

3. C.J. Patton, C.J. Design, characterization and applications of a miniature

continuous flow analysis system. Ph.D. Thesis, Mich. State U., U. Microfilms International, Ann Arbor, Mich. 150 pp (1983).

4. E.L. Atlas, S. W. Hager, L. I. Gordon, P. K. Park. *Technical Report* 215. Oregon State University, Dept. of Oceanography, Ref. No. 71-22. 48 pp. (1971).

5. W.S. Moore, R. Arnold, *J. Geophys. Res*. **101**, 1321 (1996).

6. C.J. Lorenzen, *Deep Sea Res.* **14**, 735 (1967).

7. P.H. Wiebe *et al. Mar. Biol*. **87**, 313 (1985).

8. N.M. Price *et al. Biol. Oceanogr*. **6**, 443 (1989).

9. F. Visser, L.J.A. Gerringa, S.J. Van der Gaast, H.J.W. de Baar, K.R. Timmermans, *J. Phycol.* **39**, 1085 (2003).